



## Carbon anodes for solid polymer electrolyte lithium-ion batteries

Y. Ito, M. Kawakubo, M. Ueno, H. Okuma, Q. Si, T. Kobayashi, K. Hanai, N. Imanishi\*, A. Hirano, M.B. Phillipps, Y. Takeda, O. Yamamoto

Department of Chemistry, Faculty of Engineering, Mie University, 1577 Kurimamachiyacho, Tsu, Mie 514-8507, Japan

### HIGHLIGHTS

- ▶ PEO electrolyte with high molecular weight provides low interfacial resistance to carbon anode.
- ▶ Thickness of cast carbon anode has strong influence on the kinetic performance.
- ▶ Carbon anode optimized with PEO molecular weight and thickness shows more than 300 mA g<sup>-1</sup> of reversible capacity.

### ARTICLE INFO

#### Article history:

Received 30 January 2012

Received in revised form

17 April 2012

Accepted 24 April 2012

Available online 30 April 2012

#### Keywords:

Carbon anode

Polymer electrolyte

Poly(ethylene oxide)

Lithium-ion battery

### ABSTRACT

A high specific capacity carbon anode for lithium-ion polymer batteries was developed using a mixture of a spherical mesocarbon microbeads (MCMB), vapor grown carbon fiber (VGCF), and a lithium conducting binder of polyethylene oxide (PEO) with Li(CF<sub>3</sub>SO<sub>2</sub>)<sub>2</sub>N (LiTFSI). The reversible specific capacity of the anode was dependent on the thickness of the electrode and the molecular weight ( $M_w$ ) of PEO in the composite electrode. The specific capacity of a 30 μm thick carbon anode with PEO at  $M_w = 6 \times 10^5$  was 310 mA h g<sup>-1</sup>, which was decreased to 260 mA h g<sup>-1</sup> for a 60 μm thick electrode. A reversible specific capacity of 320 mA h g<sup>-1</sup> was observed for the lithium-ion conducting binder of PEO<sub>18</sub>LiTFSI with a high  $M_w$  of  $5 \times 10^6$  and an electrode thickness of 60 μm. The specific capacity is comparable to that for a carbon anode for lithium-ion batteries using a liquid electrolyte.

© 2012 Elsevier B.V. All rights reserved.

## 1. Introduction

Large-size lithium-ion batteries have recently received much attention, due to expanding markets of electrical vehicles and for electricity storage at wind and solar power stations [1,2]. Lithium-ion batteries for such applications must be able to provide high specific energy density and excellent cyclability in addition to being safe and inexpensive [3]. Lithium-ion batteries with carbon anodes, lithium containing metal oxide cathodes such as LiCoO<sub>2</sub>, and non-aqueous liquid electrolytes exhibit high specific energy density and long-term cyclability, but the safety of large-size lithium-ion batteries is still questionable, especially in the case of abusive use. The safety of lithium-ion batteries is mainly related to the thermal reactivity of the components. The reaction heat of lithiated artificial graphite, polyvinylidene fluoride (PVdF), and non-aqueous electrolyte of 1 M LiPF<sub>6</sub> in propylene carbonate/ethylene carbonate/

dimethylene carbonate (1:1:3 volume ratio) was 1500 J g<sup>-1</sup> and 4.3 J mA h<sup>-1</sup> [4]. In contrast, a mixture of lithiated mesocarbon microbeads (MCMB) and a polyethylene oxide (PEO)-based polymer electrolyte exhibited a low reaction heat of 160 J g<sup>-1</sup> and 0.53 J mA h<sup>-1</sup> [5]. The reaction heat could be compared to that for lithium metal and PEO electrolyte of 4500 J g<sup>-1</sup> and 1.24 J mA h<sup>-1</sup> [5]. The much lower reaction heat of the MCMB electrode with a PEO-based polymer electrolyte is quite attractive for anode application in large-scale lithium-ion polymer batteries.

It has been commonly recognized that the cyclic performance of a graphite anode with a polymer electrolyte is quite poor and therefore lithium metal has been used as the anode for polymer electrolyte batteries [6]. Although lithium metal can achieve a high energy density, there are safety problems arising from dendrite formation on the anode surface [7]. Recently, Imanishi et al. [8] and Kobayashi et al. [9] reported that a spherical carbon anode material exhibits high reversible capacity for polymer electrolyte batteries, the capacity of which was comparable to that with a liquid electrolyte. These results suggest the possibility to develop a safe lithium-ion polymer battery with high energy density that is

\* Corresponding author. Tel.: +81 59 231 9420; fax: +81 59 231 9478.

E-mail address: [imanishi@chem.mie-u.ac.jp](mailto:imanishi@chem.mie-u.ac.jp) (N. Imanishi).

comparable to conventional lithium-ion batteries that employ non-aqueous liquid electrolytes.

However, it has been previously reported that the capacity of a carbon anode with a polymer electrolyte is dependent on the thickness of the electrode. A 30  $\mu\text{m}$  thick electrode had almost the same capacity as that with a liquid electrolyte, whereas the capacity of a 100  $\mu\text{m}$  thick electrode was approximately 30% that of the 30  $\mu\text{m}$  thick electrode at a charge–discharge rate of  $C/10$  [5]. It is desirable to use a thick electrode to obtain high gravimetric energy density at a high rate, because the weight of the current collector should be added to the electrode weight. The key challenge of the carbon/polymer system is the solution of the large polarization in 100  $\mu\text{m}$  or thicker electrode. Toward this goal the influence of polymer molecular weight is focused in this study to provide an insight into the polarization mechanism of thick composite polymer electrode. And appropriate molecular weight is to be revealed to have high capacity with good cycling ability.

## 2. Experimental

A composite carbon anode was prepared from a mixture of MCMB (Osaka Gas Chemical, Japan, particle size 20–30  $\mu\text{m}$ ), vapor grown carbon fiber (VGCF) (Showa Denko, Japan, 0.15  $\mu\text{m}$  diameter, 20  $\mu\text{m}$  long), and PEO (Aldrich Chem., USA)–Li(CF<sub>3</sub>SO<sub>2</sub>)<sub>2</sub>N (LiTFSI; Aldrich Chem., USA) (Li/O = 1/18). The carbon electrode was prepared according to a previously reported method [5]. LiTFSI was dissolved in anhydrous acetonitrile (AN), and then MCMB and VGCF were added to the solution. PEO was then dissolved in the mixture and stirred for 3 h. The weight ratio of MCMB, VGCF, LiTFSI, and PEO was 50:10:10:30. The anode slurry was spread on copper foil using a coating machine. The thickness of the electrode was controlled by the slurry viscosity and the coating height. The coated electrode was dried at 120 °C under vacuum for 3 h to remove AN. In some cases, PVdF (Aldrich Chem., USA,  $M_w = 5.3 \times 10^5$ ) was used as the binder instead of the lithium conducting PEO binder. All electrode preparations were carried out in an Ar-filled glove box.

The polymer electrolyte was prepared according to a previously reported method [10]. A given weight of PEO ( $M_w = 10^5$ ,  $3 \times 10^5$ ,  $6 \times 10^5$ ,  $10^6$ ,  $5 \times 10^6$  and  $7 \times 10^6$ ) and LiTFSI (Li/O = 1/18) was dissolved in AN, and then 10 wt% BaTiO<sub>3</sub> (Sakai Chemicals, Japan, 50 nm particle size) was added to the solution. After stirring overnight, the viscous solution was cast in a Teflon dish. AN was slowly evaporated in an Ar-filled glove box, and the obtained film was then further dried at 90 °C under vacuum for 8 h.

Electrode performance was examined at 60 °C using a lamination-type cell by sandwiching the composite graphite electrode cast on a copper foil current collector, the polymer electrolyte, and a lithium metal counter electrode with copper foil current collector. The cell was packed in an aluminum-laminate envelope under vacuum. The active area of the carbon electrode was 2.25 cm<sup>2</sup>. Electrode charge–discharge capacities were estimated from galvanostatic charge–discharge curves measured in the voltage range of 0.01–1.5 V using a Nagano BTS 2004H battery cycler. The charge and discharge rate was typically set at  $C/10$ . The operation temperature was 60 °C, because the room temperature conductivity of the PEO<sub>18</sub>LiTFSI polymer electrolyte was too low to apply a high current density.

The electrical conductivities of PEO<sub>18</sub>LiTFSI–BaTiO<sub>3</sub> with different molecular weight PEO were measured using a Solartron 1250 frequency analyzer with a Au/PEO<sub>18</sub>LiTFSI–BaTiO<sub>3</sub>/Au cell in the frequency range from 10<sup>6</sup> to 0.1 Hz at temperatures ranging from 25 to 80 °C. The interface resistance between the electrode and polymer electrolyte was estimated from impedance profiles of Li/PEO<sub>18</sub>LiTFSI–BaTiO<sub>3</sub>/PEO<sub>18</sub>LiTFSI–VGCF–MCMB using a frequency analyzer (Solartron 1250) with an electrochemical interface

(Solartron 1286) in the frequency range from 10<sup>6</sup> to 0.1 Hz at 60 °C. Z-plot software was employed for data analysis using a proposed equivalent circuit.

The viscoelasticity of the PEO<sub>18</sub>LiTFSI–BaTiO<sub>3</sub> film was measured as a function of the molecular weight of PEO at room temperature using an SII TMA/SS 6100 stress strain analyzer. The viscoelasticity was estimated from the stress/strain curves at 20% strain. Scanning electron microscopy (SEM) observations were made using a Hitachi S4800 FE-SEM.

## 3. Results and discussion

Fig. 1 shows the temperature dependence of the electrical conductivity of PEO<sub>18</sub>LiTFSI–10 wt% BaTiO<sub>3</sub> as a function of the molecular weight of PEO. The conductivity of PEO<sub>18</sub>LiTFSI ( $M_w = 6 \times 10^5$ )–10 wt% BaTiO<sub>3</sub> is comparable to that previously reported for PEO<sub>20</sub>LiTFSI ( $M_w = 6 \times 10^5$ )–10 wt% BaTiO<sub>3</sub> [11]. The conductivity of PEO<sub>18</sub>LiTFSI decreases slightly with increasing  $M_w$  and the activation energies for conduction show no significant change with the molecular weight of PEO. The conductivity at 60 °C was  $3.8 \times 10^{-4} \text{ S cm}^{-1}$  for PEO<sub>18</sub>LiTFSI ( $M_w = 3 \times 10^5$ )–10 wt% BaTiO<sub>3</sub> and  $2.8 \times 10^{-4} \text{ S cm}^{-1}$  for PEO<sub>18</sub>LiTFSI ( $M_w = 5 \times 10^6$ )–10 wt% BaTiO<sub>3</sub>. The conductivity has an inflection at around 45 °C, which corresponds to the solid-to-liquid phase transition [12], and slightly decreases with the decrease in the molecular weight of PEO. The activation energy for conduction in the high temperature range was 39.8 kJ mol<sup>-1</sup> for PEO<sub>18</sub>LiTFSI ( $M_w = 3 \times 10^5$ )–10 wt% BaTiO<sub>3</sub> and 38.5 kJ mol<sup>-1</sup> for PEO<sub>18</sub>LiTFSI ( $M_w = 5 \times 10^6$ )–10 wt% BaTiO<sub>3</sub>. The addition of BaTiO<sub>3</sub> into PEO<sub>18</sub>LiTFSI was effective to reduce the Li/PEO<sub>18</sub>LiTFSI interface resistance and enhance the electrical conductivity [11,13]. In this study, the composite electrolyte with 10 wt% BaTiO<sub>3</sub> in PEO<sub>18</sub>LiTFSI ( $M_w = 6 \times 10^5$ ) was typically used as the separator electrolyte.

The conductivity of PEO<sub>18</sub>LiTFSI–10 wt% BaTiO<sub>3</sub> has no significant dependence on the molecular weight of PEO, but the viscoelasticity of the composite polymer electrolyte has appreciable dependence on the molecular weight, as shown in Fig. 2, where the viscoelasticity increases with increasing molecular weight. The mechanical properties of the lithium conductive binder in the electrode composite may be an important factor in the contact formed between the MCMB, VGCF, and the binder. It is generally difficult to compare the polymer electrolyte separator with the lithium-ion conducting binder in the electrode mixture [14], and the relationship between the mechanical properties of the binder

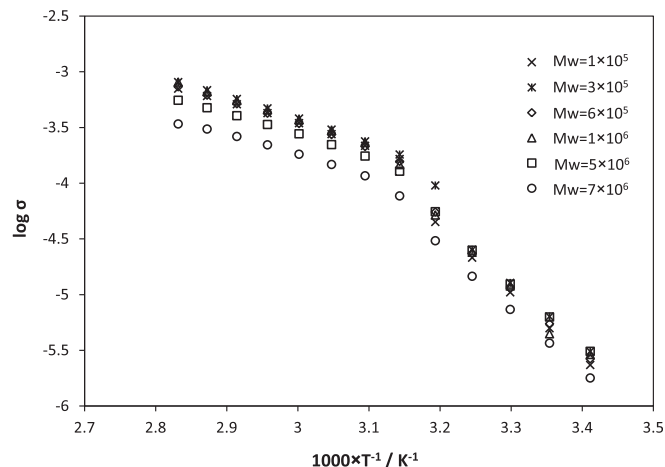


Fig. 1. Temperature dependence of the electrical conductivity of PEO<sub>18</sub>LiTFSI–10 wt% BaTiO<sub>3</sub> as a function of the molecular weight of PEO.

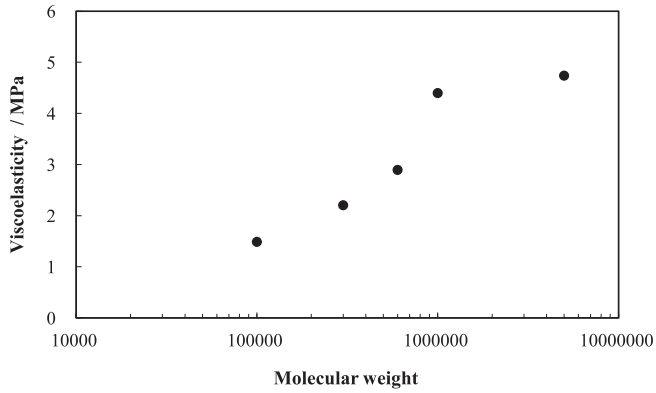


Fig. 2. Viscoelasticity of PEO<sub>18</sub>LiTFSI–10 wt% BaTiO<sub>3</sub> at room temperature as a function of the molecular weight of PEO.

and the electrode performance in lithium polymer electrolyte cells has not been reported. Therefore, the effect of the molecular weight of PEO in the composite carbon electrode on the reversible capacity was examined.

The effect of the molecular weight of PEO in a separator electrolyte of PEO<sub>18</sub>LiTFSI–10 wt% BaTiO<sub>3</sub> on the reversible capacity was examined, where the non-lithium conducting PVdF binder was used for the carbon electrode. Fig. 3 shows the charge and discharge performance of Li/PEO<sub>18</sub>LiTFSI–10 wt% BaTiO<sub>3</sub>/MCMB–VGCF–PVdF cells as a function of the molecular weight of PEO in the PEO<sub>18</sub>LiTFSI separator for two carbon electrodes with thicknesses of approximately 30 μm (ca. one layer of MCMB particles) and 60 μm (ca. two layers of MCMB particles). The charge and discharge capacity at a rate of C/10 for the 30 μm thick electrode shows no significant change due to the molecular weight of PEO in the range from 10<sup>5</sup> to 7 × 10<sup>6</sup>. The 60 μm thick carbon

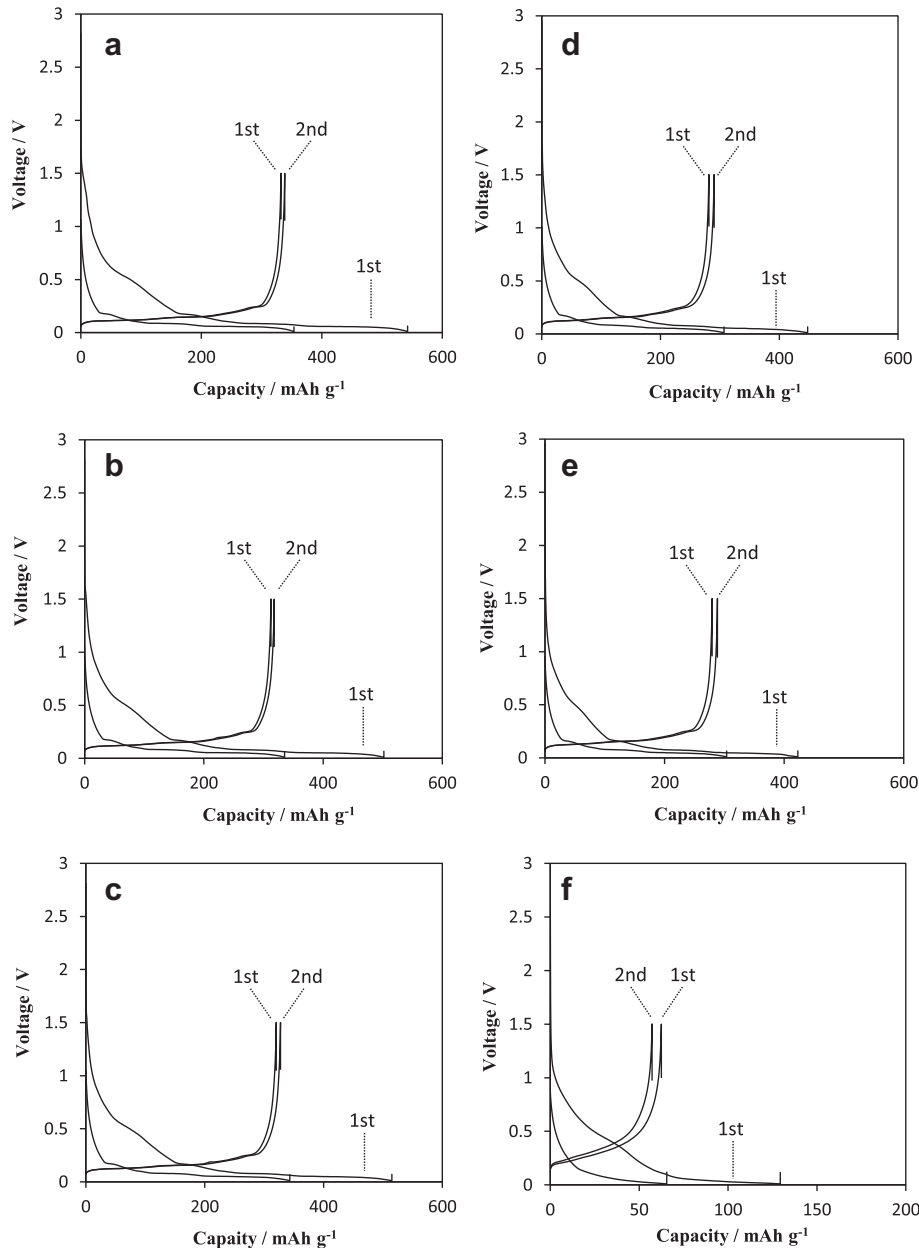


Fig. 3. Charge and discharge performance of MCMB–VGCF–PVdF/PEO<sub>18</sub>LiTFSI–10 wt% BaTiO<sub>3</sub>/Li as a function of the molecular weight of PEO at 60 °C and at a charge–discharge rate of C/10. (a)  $M_w = 1 \times 10^5$ , thickness = 30 μm, (b)  $M_w = 6 \times 10^5$ , thickness = 30 μm, (c)  $M_w = 1 \times 10^6$ , thickness = 30 μm, (d)  $M_w = 5 \times 10^6$ , thickness = 30 μm, (e)  $M_w = 7 \times 10^6$ , thickness = 30 μm, (f)  $M_w = 6 \times 10^5$ , thickness = 60 μm.

electrode with the non-lithium conductive PVdF binder shows an extremely low reversible capacity of  $52 \text{ mA h g}^{-1}$  (Fig. 3(f)). The low capacity for the thicker electrode may be due to blocking of lithium insertion into MCMB by PVdF. The addition of a lithium-ion conducting binder into the carbon electrode is essential for thick electrodes of polymer electrolyte batteries, because the electrolyte cannot penetrate into the inside of the electrode as with liquid electrolytes. Therefore, lithium conducting PEO<sub>18</sub>LiTFSI binders with different molecular weights were used in this study, and PEO ( $M_w = 6 \times 10^5$ )–10 wt% BaTiO<sub>3</sub> was used as the separator polymer electrolyte.

We have previously reported [5] the effect of the MCMB–VGCF–PEO<sub>18</sub>LiTFSI carbon anode thickness; the reversible capacity of a  $100 \mu\text{m}$  thick electrode was significantly decreased to approximately  $90 \text{ mA h g}^{-1}$  from  $310 \text{ mA h g}^{-1}$  for a  $30 \mu\text{m}$  thick electrode. The effect of the composite anode thickness on the reversible capacity of a composite anode of MCMB, PEO<sub>18</sub>LiTFSI ( $M_w = 6 \times 10^5$ ) and VGCF was examined in more detail to determine the critical electrode thickness. Fig. 4 shows typical charge–discharge curves for a Li/PEO<sub>18</sub>LiTFSI–10 wt% BaTiO<sub>3</sub>/MCMB–VGCF–PEO<sub>18</sub>LiTFSI ( $M_w = 6 \times 10^5$ ) cell as a function of the carbon composite electrode thickness at  $60^\circ\text{C}$  and at a rate of  $C/10$ . The capacity decreased significantly from  $270 \text{ mA h g}^{-1}$  for the  $60 \mu\text{m}$  thick electrode to  $120 \text{ mA h g}^{-1}$  for the  $80 \mu\text{m}$  thick electrode and to  $50 \text{ mA h g}^{-1}$  for the  $100 \mu\text{m}$  thick electrode. The particle size of MCMB is approximately  $20\text{--}30 \mu\text{m}$ ; therefore, a two-layer stack of MCMB particles may be the critical thickness to obtain a high specific capacity carbon anode with a polymer electrolyte at a rate of  $C/10$ . Fig. 5 shows SEM images of the  $30$  and  $100 \mu\text{m}$  thick composite electrodes coated on copper foil. The MCMB particles are distributed homogeneously throughout the polymer electrolyte and VGCF matrix. Most of the MCMB particles could contact directly with the polymer electrolyte separator for the  $30 \mu\text{m}$  thick electrode, but only one-third of the MCMB particles for the  $100 \mu\text{m}$  thick electrode. Therefore, the interface between MCMB particles and the polymer electrolyte in the electrode would be a significant factor that affects cell performance.

The electrode impedance of the composite electrode provides useful information regarding electrode performance. The impedance of Li/PEO<sub>18</sub>LiTFSI–10 wt% BaTiO<sub>3</sub>/MCMB–VGCF–PEO<sub>18</sub>LiTFSI ( $M_w = 6 \times 10^5$ ) at  $60^\circ\text{C}$  was examined as a function of electrode thickness. Fig. 6 shows two semicircles in the impedance profiles, where the carbon electrode potential was fixed at  $800 \text{ mV vs. Li}$  in Fig. 6(a–c), and at  $10 \text{ mV}$  in Fig. 6(d). Impedance analysis of the Li/PEO<sub>18</sub>LiTFSI–10 wt% BaTiO<sub>3</sub>/Li cell indicates the effect of Li/PEO<sub>18</sub>LiTFSI–10 wt% BaTiO<sub>3</sub>/MCMB–VGCF–PEO<sub>18</sub>LiTFSI

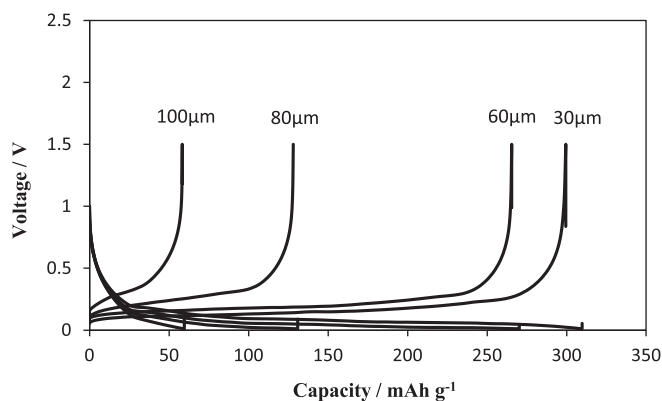


Fig. 4. Charge–discharge curves for MCMB–PEO<sub>18</sub>LiTFSI ( $M_w = 6 \times 10^5$ )–VGCF/PEO<sub>18</sub>LiTFSI–10 wt% BaTiO<sub>3</sub>/Li as a function of the electrode thickness after 3 cycles at  $60^\circ\text{C}$  and at charge–discharge rate of  $C/10$ . Cut-off voltage:  $10\text{--}1500 \text{ mV}$ .

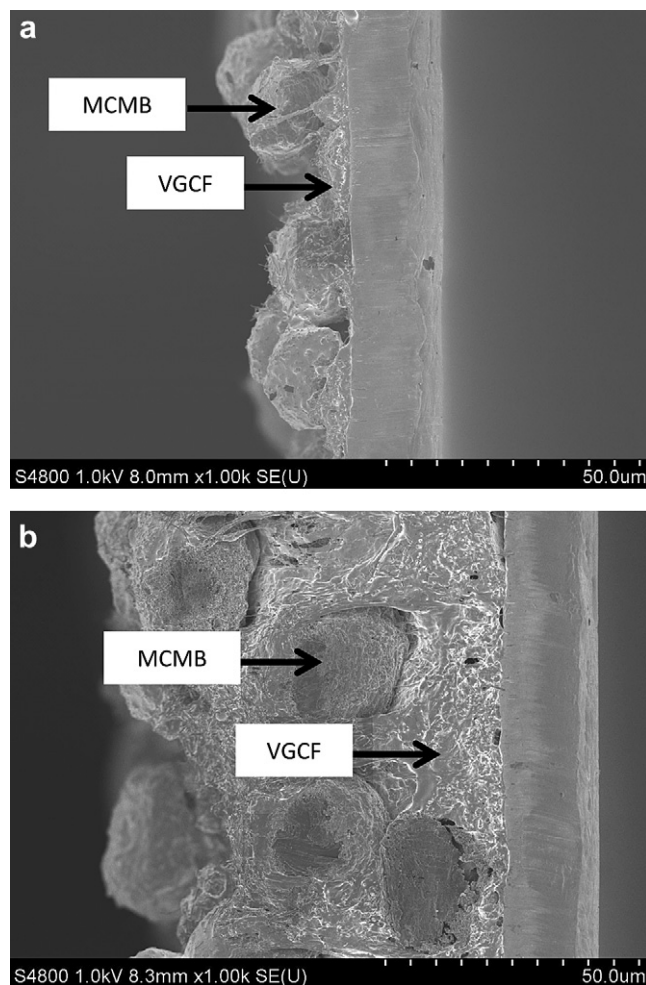
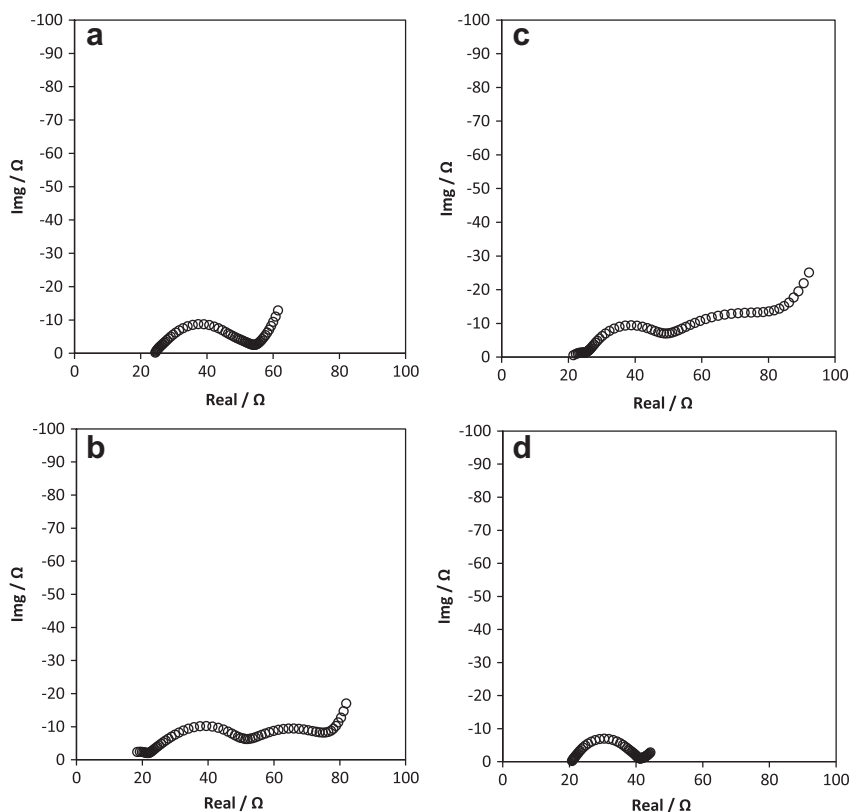


Fig. 5. Cross-sectional SEM images of the (a)  $30$  and (b)  $100 \mu\text{m}$  thick MCMB–PEO<sub>18</sub>LiTFSI ( $M_w = 6 \times 10^5$ )–VGCF electrodes coated on copper foil.

( $M_w = 6 \times 10^5$ ) on the electrode potential; the high frequency semicircle corresponds to the interface resistance between lithium metal and the polymer electrolyte, and the low frequency semicircle indicates that between the carbon electrode and the polymer electrolyte. The low frequency semicircle was diminished with the decrease in the carbon electrode potential, as shown in Fig. 6(d) but reappeared again with increase in the carbon electrode potential. Therefore, the low frequency semicircle most likely corresponds to the charge transfer resistance between the carbon electrode and the polymer electrolyte, and the interface layer resistance between carbon and the polymer electrolyte may be small. The charge transfer resistance increased with decreasing lithium content in the carbon electrode and with increasing electrode thickness. The charge transfer resistance for the  $80$  and  $100 \mu\text{m}$  thick electrodes at  $800 \text{ mV vs. Li}$  was much larger at  $60 \Omega \text{ cm}^2$  and  $135 \Omega \text{ cm}^2$ , respectively, than  $22.5 \Omega \text{ cm}^2$  for the  $30 \mu\text{m}$  thick electrode. It is not clear why the charge transfer resistance increases with the electrode thickness, because the reaction area for lithium-ion transport increases with the electrode thickness, as shown in Fig. 5. The reversible capacity of the electrode is dependent on the current density. The capacity of the composite electrodes in Fig. 4 was measured at a rate of  $C/10$  and the packing density of the composite anodes was also dependent on the electrode thickness, and so the packing density of the composite electrode increased with increasing electrode thickness. The current densities per  $\text{cm}^2$  for



**Fig. 6.** Impedance profiles of MCMB–PEO<sub>18</sub>LiTFSI ( $M_w = 6 \times 10^5$ )/PEO<sub>18</sub>LiTFSI–10 wt% BaTiO<sub>3</sub>/Li measured at 60 °C as a function of the electrode thickness. (a) Electrode potential = 800 mV, electrode thickness = 30  $\mu\text{m}$ . (b) Electrode potential = 800 mV, electrode thickness = 60  $\mu\text{m}$ . (c) Electrode potential = 800 mV, electrode thickness = 100  $\mu\text{m}$ . (d) Electrode potential = 10 mV, electrode thickness = 30  $\mu\text{m}$ .

the electrode contact area with the polymer electrolyte separator were 0.073 and 0.49 mA cm<sup>-2</sup> for the 30 and 100  $\mu\text{m}$  thick electrodes, respectively. Therefore, more current may pass through the boundary of the polymer electrolyte separator and anode composite for a thicker electrode. The low specific capacity of the 100  $\mu\text{m}$  thick electrode could be explained by the high interface resistance and high packing density.

One of the important requirements for the practical use of lithium-ion polymer batteries is a high specific capacity at a high charge and discharge rate. The carbon electrode thickness is an important factor to obtain a high energy density carbon anode, including the weight of the copper current collector. The effect of lithium salts such as LiTFSI, LiC<sub>2</sub>F<sub>5</sub>(SO<sub>2</sub>)<sub>2</sub>N, LiB(C<sub>2</sub>O<sub>4</sub>)<sub>2</sub> and LiClO<sub>4</sub> in the lithium conducting PEO binder was examined. The lowest carbon electrode interface resistance and the highest reversible capacity were observed for LiTFSI in PEO. In addition, higher molecular weight PEO in the binder of the carbon anode improved the reversible capacity of the thick electrode. Fig. 7 shows the charge–discharge curves at the 3rd cycle for Li/PEO<sub>18</sub>LiTFSI–10 wt% BaTiO<sub>3</sub>/MCMB–VGCF–PEO<sub>18</sub>LiTFSI as a function of the molecular weight of PEO in the carbon electrode for 60 and 100  $\mu\text{m}$  thick electrodes. The effect of the PEO molecular weight on the 60  $\mu\text{m}$  thick electrode is evident. A reversible capacity of 320 mA h g<sup>-1</sup>, which is comparable to that of a carbon anode with a liquid electrolyte [5], is observed for PEO with a molecular weight of  $5 \times 10^6$ , although no significant increase in the capacity (C/10 rate) of the 100  $\mu\text{m}$  thick electrode was evident by increasing the molecular weight of PEO. However, at a charge–discharge rate as low as C/20, the reversible capacity was approximately 300 mA h g<sup>-1</sup> for the 100  $\mu\text{m}$  carbon anode with PEO having  $M_w = 5 \times 10^6$ . The high capacity of the 60  $\mu\text{m}$  thick electrode with a high molecular weight PEO could explain the low carbon electrode charge transfer

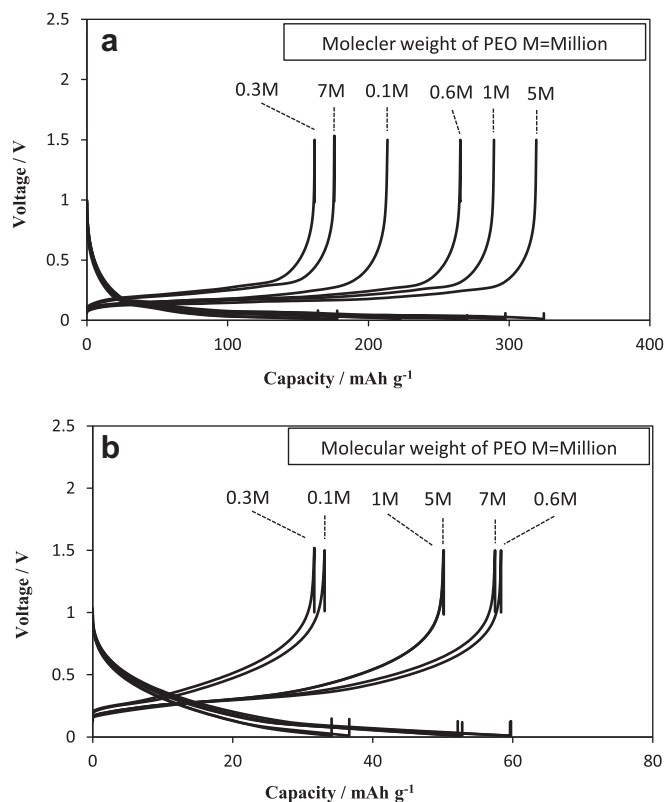


**Fig. 7.** Charge–discharge curves of MCMB–PEO<sub>18</sub>LiTFSI–VGCF/PEO<sub>18</sub>LiTFSI–10 wt% BaTiO<sub>3</sub>/Li at the 3rd cycle as a function of the PEO molecular weight in the electrode at 60 °C and at a charge–discharge rate of C/10. Cut-off voltage: 10–1500 mV. (a) Electrode thickness = 60  $\mu\text{m}$ . (b) Electrode thickness = 100  $\mu\text{m}$ .

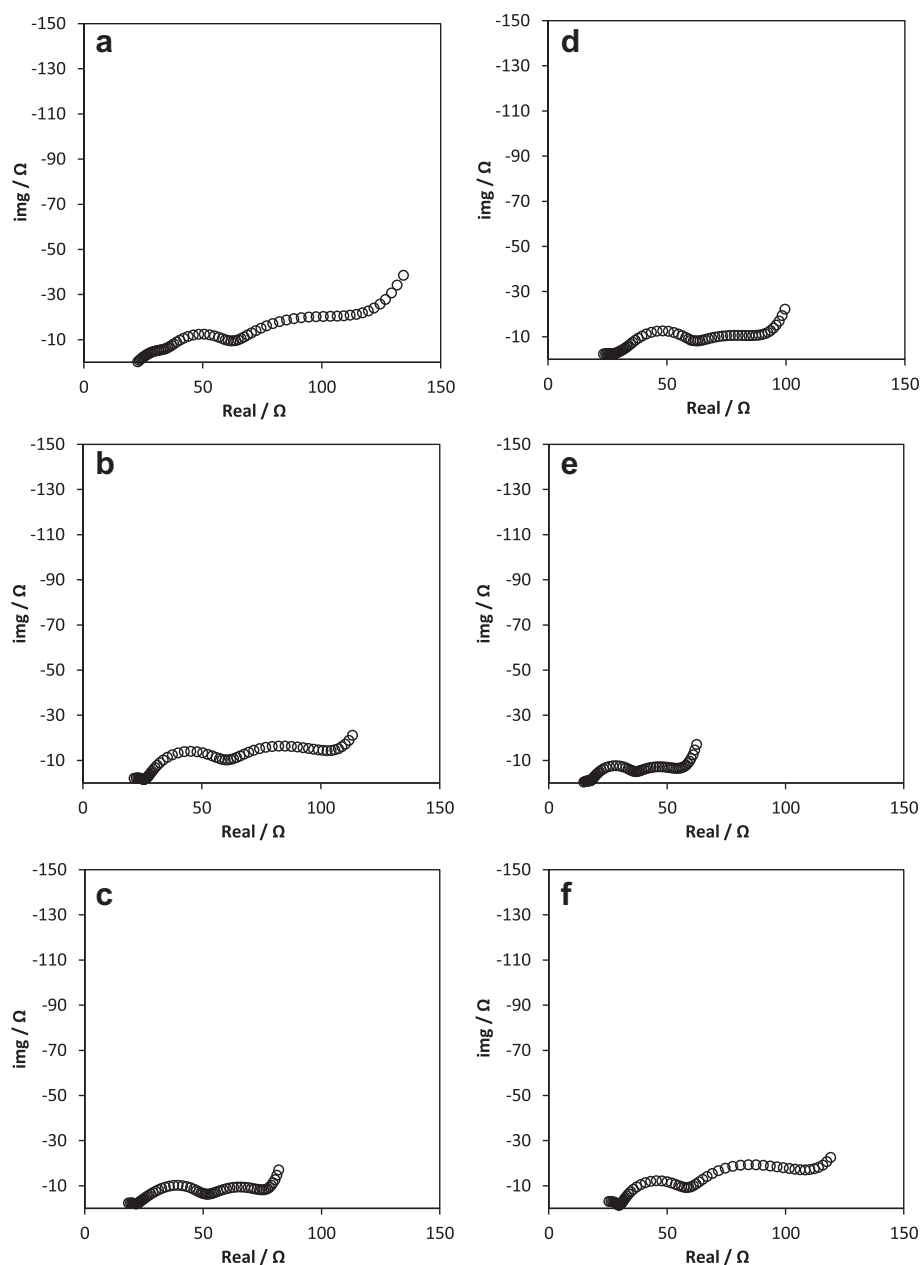


**Fig. 8.** Impedance profiles of MCMB–PEO<sub>18</sub>LiTFSI–VGCF/PEO<sub>18</sub>LiTFSI–BaTiO<sub>3</sub>/Li as a function of the molecular weight of PEO in the electrode at 60 °C, where the thickness of the electrode is approximately 60 μm. (a)  $M_w = 1 \times 10^5$ , (b)  $M_w = 3 \times 10^5$ , (c)  $M_w = 6 \times 10^5$ , (d)  $M_w = 1 \times 10^6$ , (e)  $M_w = 5 \times 10^6$ , and (f)  $M_w = 7 \times 10^6$ .

**Table 1**

Reversible capacity (Cap.), charge–discharge efficiency at the first cycle (Eff.), and interface resistance between the carbon electrode and polymer electrolyte (Res.) of the MCMB–VGCF–PEO<sub>18</sub>LiTFSI composite electrode at 60 °C and at a charge–discharge rate of C/10.

PEO $M_w$	Electrode thickness											
	30 μm			60 μm			80 μm			100 μm		
	Cap. (mA h g <sup>-1</sup> )	Eff. (%)	Res. (Ω cm <sup>2</sup> )	Cap. (mA h g <sup>-1</sup> )	Eff. (%)	Res. (Ω cm <sup>2</sup> )	Cap. (mA h g <sup>-1</sup> )	Eff. (%)	Res. (Ω cm <sup>2</sup> )	Cap. (mA h g <sup>-1</sup> )	Eff. (%)	Res. (Ω cm <sup>2</sup> )
100,000	307	72		210	80	106	129			32	36	
300,000	304	77		170	80	104	154			32	41	
600,000	310	76	22.5	260	82	61	105		90	50	51	135
1,000,000	279	80		280	86	74	105			50	51	
5,000,000	340	81		320	87	50	161			50	57	
7,000,000	327	71		170	81	117	96			58	58	

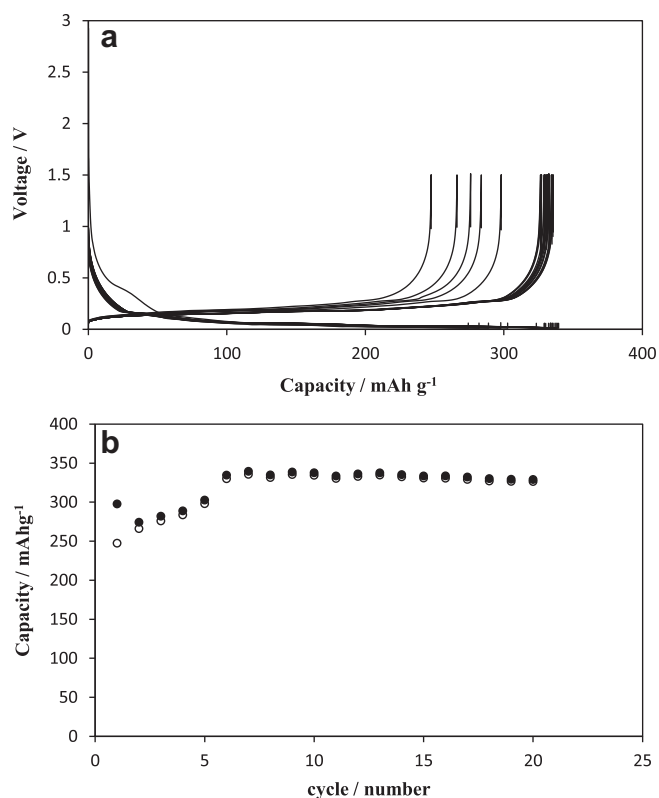


**Fig. 9.** (a) Charge–discharge curves and (b) capacity change with cycling for MCMC–PEO<sub>18</sub>LiTFSI ( $M_w = 5 \times 10^6$ )–VGCF/PEO<sub>18</sub>LiTFSI–BaTiO<sub>3</sub>/Li at 60 °C and at a charge–discharge rate of C/10, where the thickness of the carbon electrode is 60  $\mu\text{m}$ . Cut-off voltage: 10–1500 mV, ●: lithium insertion, ○: lithium deinsertion.

resistance of the carbon electrode with high molecular weight PEO, as shown in Fig. 8. A decrease in the charge transfer resistance in the carbon composite electrode was observed with an increase in the molecular weight of PEO up to  $5 \times 10^6$ . It is not clear why the carbon electrode with high molecular weight PEO exhibits low charge transfer resistance, but one possibility is that the contact between the carbon particles and lithium conducting binder is improved when PEO with suitable viscoelasticity is employed. An irreversible capacity was observed in the first lithium insertion and deinsertion process. The irreversible capacity corresponds to the formation of a solid electrolyte interface (SEI) [14]. The efficiency of the first charge–discharge cycle for the 60  $\mu\text{m}$  thick electrode increased from 80% for PEO with  $M_w = 3 \times 10^5$  to 87% for PEO with  $M_w = 5 \times 10^6$ . These results suggest that high molecular weight PEO results in a thinner SEI film on the surface of MCMC. The SEI may have good characteristics for the charge transfer reaction with lithium ions. In Table 1, the reversible capacity, first cycle charge–discharge efficiency, and the interface resistance between the carbon composite electrode and PEO electrolyte are summarized as a function of the electrode thickness and the molecular weight of PEO in the carbon electrode.

The cyclic performance of the 60  $\mu\text{m}$  thick carbon electrode with PEO of  $5 \times 10^6$  was examined. Fig. 9 shows the cyclability for the

MCMC–PEO<sub>18</sub>LiTFSI ( $M_w = 5 \times 10^6$ )–VGCF/PEO<sub>18</sub>LiTFSI–BaTiO<sub>3</sub>/Li cell with the 60  $\mu\text{m}$  thick carbon electrode at 60 °C and at a rate of C/10. A reversible capacity of 330 mA h g<sup>-1</sup>, which is comparable to that for a carbon anode in liquid electrolyte, was observed for more than 20 cycles, and the degradation of capacity by cycling was very low. The carbon electrode with high molecular weight PEO electrolyte exhibited excellent electrode performance at C/10. However, this electrode had a low lithium insertion capacity at a high rate of C/2, which indicates that the interface between the carbon and the polymer electrolyte requires further improvement to obtain higher capacity at a high charge–discharge rate.

#### 4. Conclusions

The lithium-ion conducting binder of PEO<sub>18</sub>LiTFSI was examined as a function of the molecular weight of PEO with an aim to improve the specific capacity of a thick MCMC carbon anode with a polymer electrolyte. The reversible capacity of the carbon anode was increased to 320 mA h g<sup>-1</sup> by increasing the molecular weight of PEO up to  $5 \times 10^6$  for a 60  $\mu\text{m}$  thick electrode, which is comparable to that for a carbon anode with a liquid electrolyte. The MCMC–VGCF–PEO<sub>18</sub>LiTFSI ( $M_w = 5 \times 10^6$ ) composite electrode showed excellent cycling performance with a high reversible capacity. The high capacity of the carbon electrode with a high molecular weight PEO<sub>18</sub>LiTFSI ( $M_w = 5 \times 10^6$ ) lithium conducting binder could be explained the low interface resistance of the SEI formed between carbon and the polymer electrolyte due to improved contact of MCMC with VGCF and the PEO<sub>18</sub>LiTFSI matrix.

#### Acknowledgments

This study was partly supported by the Cooperation of Innovative Technology and Advanced Research in Evolution Area (City Area) Project of the Ministry of Education, Culture, Sports, Science and Technology of Japan.

#### References

- [1] P.G. Bruce, *Solid State Ionics* 179 (2008) 752.
- [2] G. Girishkumar, B. McCloskey, A.C. Luntz, S. Swanson, W. Wilcke, *J. Phys. Chem. Lett.* 1 (2000) 2193.
- [3] B. Scrosati, *Chem. Rec.* 1 (2001) 173.
- [4] P. Biensan, B. Simon, J.P. Peres, A. de Guibert, M. Broussely, J.M. Bodet, F. Pertion, *J. Power Sources* 81–82 (1999) 906.
- [5] D. Saito, Y. Ito, K. Hanai, T. Kobayashi, N. Imanishi, A. Hirano, Y. Takeda, O. Yamamoto, *J. Power Sources* 195 (2010) 6172.
- [6] B. Scrosati, F. Croce, S. Panero, *J. Power Sources* 100 (2001) 93.
- [7] C. Brisson, M. Rosso, J.N. Chazalviel, S. Lascaud, *J. Power Sources* 81–82 (1999) 925.
- [8] N. Imanishi, Y. Ono, K. Hanai, R. Uchiyama, Y. Liu, A. Hirano, Y. Takeda, O. Yamamoto, *J. Power Sources* 178 (2008) 744.
- [9] Y. Kobayashi, S. Seki, Y. Mita, Y. Ohno, H. Miyashiro, P. Charest, A. Guerfi, K. Zaghbi, *J. Power Sources* 185 (2008) 542.
- [10] C. Capiglia, J. Yang, N. Imanishi, A. Hirano, Y. Takeda, O. Yamamoto, *J. Power Sources* 119–121 (2003) 826.
- [11] H.Y. Sun, Y. Takeda, N. Imanishi, O. Yamamoto, H.-J. Sohn, *J. Electrochem. Soc.* 147 (2000) 2462.
- [12] A. Vallée, S. Besner, J. Prud'Homme, *Electrochim. Acta* 37 (1992) 1579.
- [13] T. Zhang, N. Imanishi, S. Hasegawa, A. Hirano, J. Xie, Y. Takeda, O. Yamamoto, N. Sammes, *Electrochem. Solid-State Lett.* 12 (2009) A132.
- [14] J.O. Besenhard, M. Winter, J. Yang, W. Biberacher, *J. Power Sources* 54 (1995) 228.